

The Eurasia Proceedings of Science, Technology, Engineering & Mathematics (EPSTEM), 2023

Volume 22, Pages 348-358

ICBASSET 2023: International Conference on Basic Sciences, Engineering and Technology

NMR Spin Echo Study of Domain Wall Pinning in Magnets in Combination with an Additional Magnetic Video-Pulse

Tsisana GAVASHELI

Ivane Javakhishvili Tbilisi State University

Grigor MAMNIASHVILI

Ivane Javakhishvili Tbilisi State University

Tatiana GEGECHKORI

Ivane Javakhishvili Tbilisi State University

Abstract: NMR spin echo at application of an additional magnetic video-pulse is a convenient method to study the domain wall pinning in magnetic materials. Domain wall (DW) pinning is the critical amplitude of the magnetic video-pulse (MVP) below which the DW is fixed. For its assessment, two alternative NMR methods were chosen. In the first case, the pinning of DW was measured by the action of MVP on a two-pulse echo signal, and in the second one, the pinning was measured at the combined action of MVP and radiofrequency (RF) pulses on the nuclear spin system in DW during the process of formation a single-pulse echo, by means of generation of the so-called magnetic echo signal. DW pinning was studied by these two methods in magnets (lithium-zinc ferrite and cobalt micropowder samples).

Keywords: Nuclear spin echo, Magnetic video-pulse, Two-pulse echo, Domain wall mobility, Pinning.

Introduction

Nuclear magnetic resonance (NMR) in magnets is currently a powerful microscopic method for characterizing various magnetic materials (Turov & Petrov, 1972; Wurmehl & Kohlhepp, 2008; Shmyreva, et al., 2016; Mamniashvili et al., 2016). One of its advantages is the ability to give valuable information about the properties of domain walls (DWs). The inclusion of additional magnetic video- pulses (MVP), capable of causing the DW displacement, makes it possible to study the DW pinning, expanding the potential of the NMR method.

In particular, it was shown in (Pleshakov et al., 2016; Gavasheli et al., 2020), that the use of nuclear spin echoes from nuclei in DWs of lithium ferrite and cobalt nanowires in combination with magnetic video-pulse (MVP) is a convenient method for studying the pinning of DWs in these systems. This method is also of a great interest for the study of magnets for applications in information recording devices and sensors. For the first time, the dynamics of DW under the action of an MVP in a single-crystal of a ferrite sample was investigated by Galt (Galt, 1954). It was shown that the dynamics of DW is described by the linear dependence of the DW velocity v on the applied MVP:

$$v=S(H-H_0)$$

where S is the mobility of the DW and H_0 is the DW pinning - the critical field below which the DW is fixed.

The original technique of MVP exposure was used in (Pleshakov et al., 2016), which consisted in exposing of the nuclear spin system in the lithium-zinc ferrite sample with a sequence of two pairs of RF pulses in

- This is an Open Access article distributed under the terms of the Creative Commons Attribution-Noncommercial 4.0 Unported License, permitting all non-commercial use, distribution, and reproduction in any medium, provided the original work is properly cited.

- Selection and peer-review under responsibility of the Organizing Committee of the Conference

combination with an additional long-term MVP. The effect of MVP was investigated by the effect on the signals of stimulated and two-pulse echoes (TPE) formed when three or two pulses, correspondingly, are combined in the sequence. In this case, the MVP overlapped, respectively, the second and the third radiofrequency (RF) pulses, as well as the intervals between them and the signals, respectively, of the stimulated and two-pulse echoes. Under the applied MVP the echo signals are suppressed due to the inhomogeneous phase changes of rephasing nuclear isochromates which are proportional to the DW displacements and hyperfine field (HFF) anisotropy. Figure. 1a shows the result of the combined action of the MVP on the TPE signals at zero magnetic field (I) and the external magnetic field $H_e = 1000$ Oe (2), Figure 3 (Pleshakov et al., 2016), and Figure 1b shows a modified by us Figure 1a, taking into account the existence of pinning field H_0 (I) and using the same experimental points as in Figure 1a.

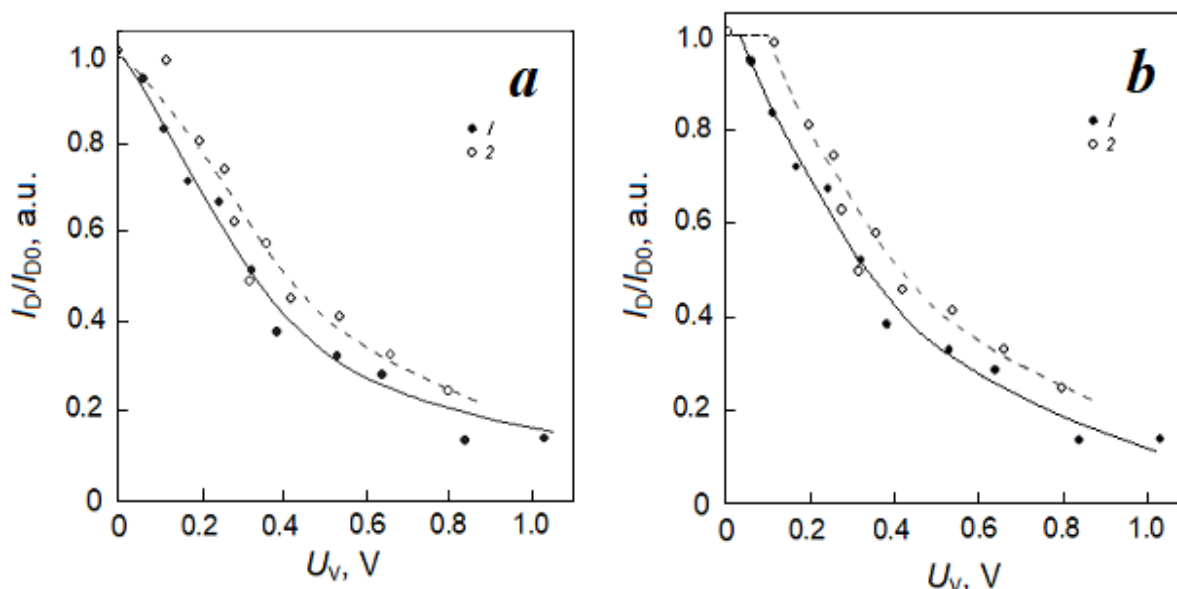


Figure 1. (a) - The dependence of the normalized amplitude of the two-pulse echo (TPE) signal on the amplitude of the magnetic video-pulse (MVP) (Pleshakov et al., 2016). (b) – The modified dependence of the normalized TPE amplitude (a) on the amplitude of the MVP. 1 - $H_e = 0$ Oe; 2 - $H_e = 1000$ Oe.

A similar effect of the MVP action on the stimulated echo was also shown in (Pleshakov et al., 2016). The dependence modified in this way shows that the results obtained in (Pleshakov et al., 2016) also indicate the possibility of measuring the pinning field H_0 of the DW, which is determined by the MVP amplitude, below which DWs are pinned and motionless. The aim of our further research is an alternative proof by two NMR methods: by the MVP action on TPE and by the combined action of RF and MVP, of the presence of DW pinning field H_0 , corresponding to the MVP amplitude below which DW is fixed.

The methodology of (Mamniashvili et al., 2015; Pleshakov et al., 2016; Gavasheli et al., 2020) is used for the study of the dependence of the pinning force H_0 in cobalt micropowders on the duration of MVP τ_m and the magnitude of the external magnetic field H_e . As it known (Mamniashvili et al., 2015), cobalt and lithium-zinc ferrite are very different in their NMR properties: in cobalt, the anisotropy of the hyperfine field (HFF) is an order of magnitude higher than its value for lithium ferrite. In addition, the value of the NMR amplification factor η in lithium ferrite is about 10^3 times higher than the value of amplification factor η in cobalt, which indicates a much greater mobility of DWs in lithium-zinc ferrite as compared to cobalt. We can obtain a preliminary estimate of the dependence of H_0 on the length of MVP from Figure 2, obtained on the basis of Figure 2 from Rassvetalov and Levitski (1981), if it is modified similarly to Figure 1 from (Gavasheli et al. (2021) or Figure 1 from Gavasheli et al. (2022), taking into account the presence of pinning force H_0 .

Figure 2 shows the dependence of TPE (for A-sites of nickel ferrite) on the duration of MVP at $H = 2(I), 4(2), 10$ Oe (3). Analysis of the dependence of H_0 on τ_m in this figure shows that for τ_m and H_0 (representing the intersection points of dependences 1, 2 and 3 with the axis τ_m in Fig. 1), the relation $A_m = H_0 \cdot \tau_m = \text{const}$, holds for all H , i.e. the pinning force H_0 is inversely proportional to τ_m . The value A_m , which is the area of the MVP, is constant for all threshold values of τ_m , when the TPE intensity begins to decrease due to the tear-off from the pinning centers.

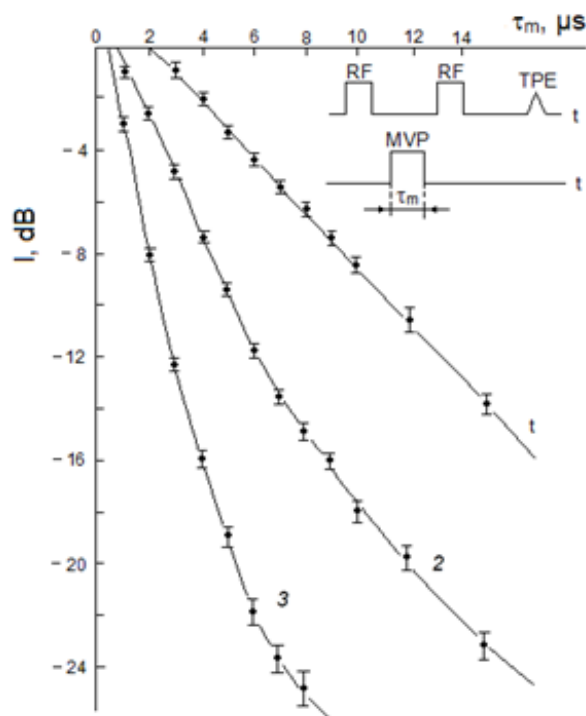


Figure 2. Dependence of TPE (A –sites of nickel ferrite) on the duration of MVP τ_m at $H = 2$ Oe (1), 4 Oe (2), 10 Oe (3).

We also note that earlier in (Mamniashvili et al., 2015; Pleshakov et al., 2016; Gavasheli et al., 2020) the dependence of H_0 on the external magnetic field H_e was not studied. As is known (Pleshakov et al., 2016), the application of a large constant magnetic field reduces the number of DWs, and the remaining ones are distributed over pinning centers, which contribute to a greater pinning. The purpose of this work is to study the experimental dependence of H_0 on τ_m and H on the example of the effect of MVP on the TPE and ME signals observed from ^{59}Co nuclei in the DWs of a cobalt micropowder.

Experimental Results and Their Discussion

The block diagram of the experimental setup is shown in Figure 3: RF excitation pulses are generated by generator 1. Next, a sequence of NMR excitation echo pulses is fed into resonator 2 with the ring-shaped lithium ferrite sample used. The RF field of the pulses excites the echo signal in the upper coil of the resonator 2. Then these pulses, together with the echo signal S , enter the receiver 3 and are recorded by the oscilloscope 4. The channel 5 generates MVP pulses applied to the lower winding of the resonator. A description of the NMR spectrometer and MVP unit is given in (Gavasheli et al., 2020). The experimental results were obtained at $T = 77$ K. The echo signal amplitude was measured in the presence and absence of a MVP with amplitude H .

We used samples of lithium-zinc ferrite $\text{Li}_{0.5}\text{Fe}_{1.0}\text{Zn}_{0.15}\text{O}_4$, which were rings with a diameter of 12-15 mm and a weight of 5-8 g, enriched in the ^{57}Fe isotope to 96.8% in order to increase the intensity of the echo signal (Mamniashvili et al., 2015). The NMR spectrum of lithium ferrite at $T = 77$ K consists of two well-resolved lines, where the low-frequency line belongs to the tetrahedral sites A, and the high-frequency line to the octahedral sites B. The ^{57}Fe NMR spectrum of the spin echo of the polycrystalline sample of lithium-zinc ferrite under study is shown in Figure 4.

Because of the large angles of electronic magnetization M rotation associated with DW displacement, the displacement of the DW under the action of MVP in between RF pulses, even being insignificant, can be accompanied by a large rotation of M . In this case, the rotation of M inside the DW is proportional to the displacement of the DW. This process is accompanied by abrupt inhomogeneous changes of dephasing isochromate frequencies proportional to the displacement of the DW due to anisotropy of the HFF in magnetic material (Gavasheli et al., 2020), resulting in the echo signal suppression.

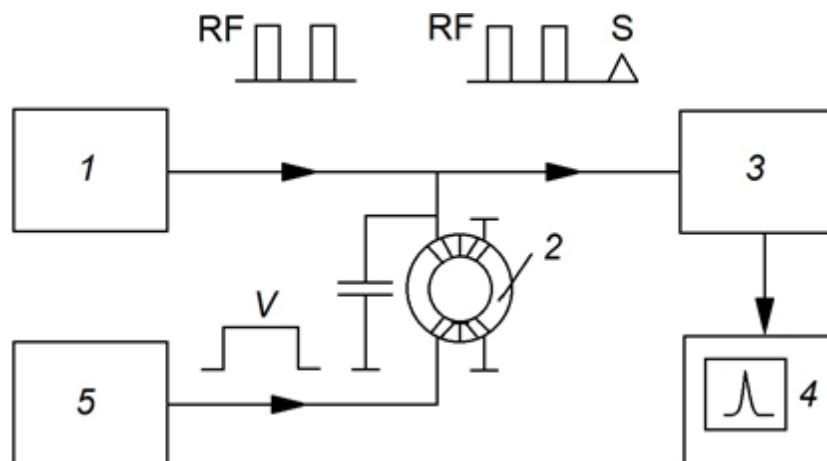


Figure 3. Block diagram of the experimental setup: 1 - RF pulse excitation generator; 2 - resonator with a ring-shaped sample of lithium-zinc ferrite; 3 - RF receiver; 4 - oscilloscope; 5 - channel of formation of MVP.

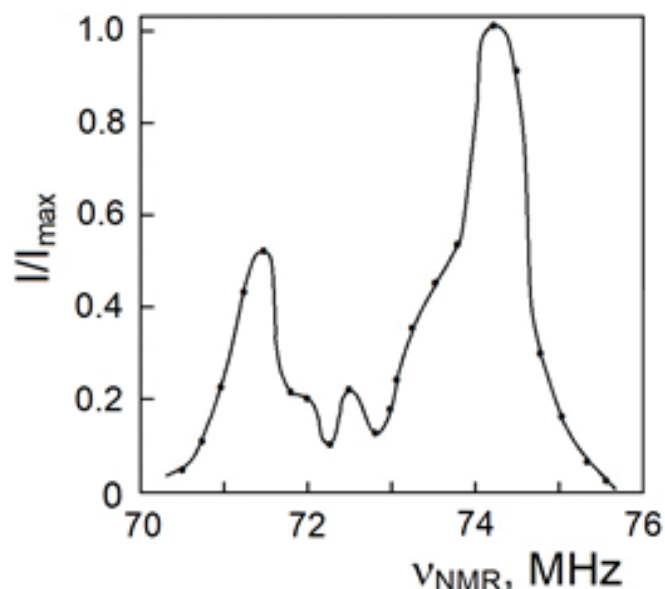


Figure 4. NMR spectrum of ^{57}Fe nuclei in polycrystalline lithium-zinc ferrite, $T = 77\text{ K}$.

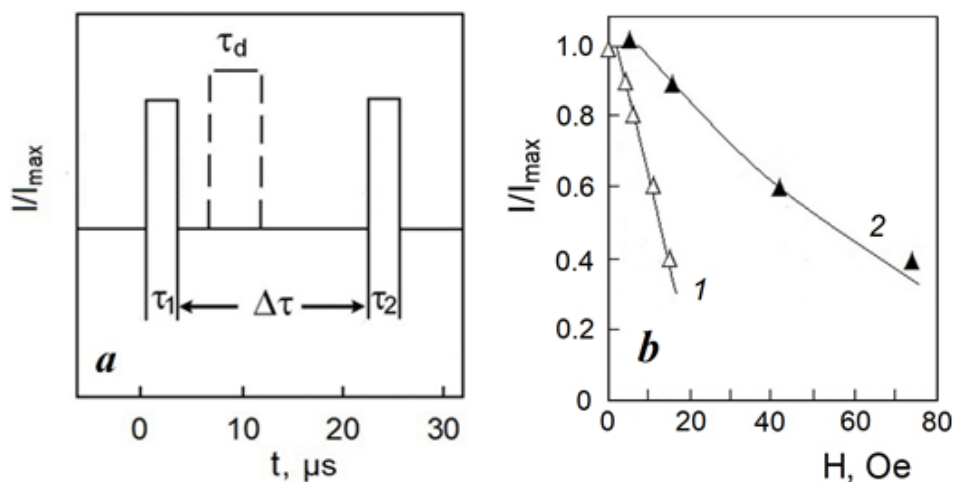


Figure 5. (a) - Position of the MVP acting in the interval between RF pulses. (b) Amplitude diagrams of the effect of MVP on a two-pulse echo (TPE) in lithium-zinc ferrite at frequencies of 71 and 74 MHz, curves – 2 and 1, corresponding to A and B positions respectively, the duration of the MVP $\tau_d = 1.0\ \mu\text{s}$, $T = 77\text{ K}$.

The MVP amplitude at which the TPE intensity begins to decline, associated with the onset of the DW motion, is naturally related to the DW pinning field H_0 . The diagram showing the effect of MVP acting in the time interval between two RF pulses on TPE is presented in Figure 5. In Figure 5b one can see also a significant increase in the pinning field H_0 upon passing from octahedral B to tetrahedral A positions.

Analysis of the dependence of the MVP effect on echo signals in the studied samples shows a significant, up to one order of magnitude, increase in DW mobility and a decrease in the pinning force in lithium ferrite as compared to cobalt (Gavasheli et al., 2020). A particularly large MVP effect on the TPE is observed for the echo signal from nuclei located in octahedral B-sites of lithium ferrite at a frequency of 74 MHz with a higher anisotropy HFF (Doroshev et al., 1972), compared to the echo from the nuclei in tetrahedral positions A at a frequency of 71 MHz, Figure 5b.

The pinning field H_0 could be measured also at the combined action of MVP and radiofrequency (RF) pulse on the nuclear spin system in DW at the process of formation a single-pulse echo (SPE), by means of generation of the so-called stimulated magnetic echo (ME) signal (Gavasheli et al., 2020). The ME is formed at combined application of RF and MVP pulses due to an abrupt non-adiabatic change of effective magnetic field

$$\vec{H}_{\text{eff}} = \frac{1}{\gamma_n} (\Delta \omega_j \vec{z} + \omega_1 \vec{y})$$

in the rotating coordinate system (RCS), where γ_n is the nuclear gyromagnetic ratio,

\vec{z} and \vec{y} are unit vectors in RCS, $\Delta \omega_j = \omega_{\text{NMR}} - \omega_{\text{RF}}$ is the detuning for the j -th isochromate, $\omega_1 = \gamma_n \eta H_1$ is the pulse amplitude in frequency units and η is the RF field amplification factor. In this case the application of MVP is equivalent to the application of additional RF pulse which in combination with two other RF pulse analogs, corresponding to the RF pulse edges, forms a ME signal (Gavasheli et al., 2020). In lithium ferrite, the oscillogram of the observed signal of a stimulated ME followed by the single-pulse echo (SPE) signal is shown at 71 MHz in Figure 6a, and dependences of ME and SPE intensities on the MVP amplitude were obtained, Figure 6b, similar to the corresponding dependences in cobalt (Gavasheli et al., 2020).

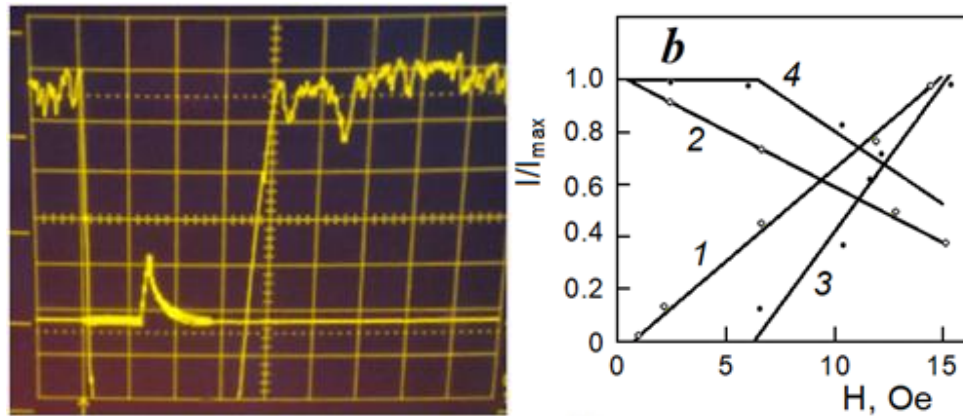


Figure 6. (a) Oscillogram of the magnetic and subsequent SPE echo signals in lithium-zinc ferrite (upper beam), NMR = 71 MHz, T = 77 K, the lower beam shows the duration of the radio frequency magnetic pulses as well as the amplitude of the magnetic video-pulse; (b) dependences of the signals of the magnetic (1,3) and single-pulse (2,4) echoes on the amplitude of the magnetic video pulse at frequencies of 74 and 71 MHz, respectively:

$$\tau_{\text{RF}} = 15 \mu\text{s}, \tau_d = 0.5 \mu\text{s}, T = 77 \text{ K}.$$

The amplitude of MVP at which the ME appears, Figure 6b, correlates with the MVP amplitude acting on the TPE, at which its decrease begins, which is associated with the DW pinning field H_0 , Fig. 4b, giving an alternative way to measure DW pinning force H_0 and mobility in magnets.

The observed experimental dependences of the SPE and TPE signals can be understood taking into account that, according to (1), under the action of the MVP, the DW reversibly shifts at a distance Δx proportional to the MVP amplitude $\Delta x \sim v \tau_d = S (H - H_0) \tau_d$, when the MVP amplitude exceeds the values of the pinning field H_0 . In the Δx layer, the nuclei under the combined action of RF and MVP experience the effect of a jump-like change in the magnitude and direction of the effective magnetic field H_{eff} in the RCS, due to the corresponding change in the local HFF and factor η . Therefore, according to the nonresonant model of the SPE formation (Gavasheli et al., 2020), the effect of the MVP is equivalent to the effect of the second RF pulse in combination

with two RF pulse analogs corresponding to the RF pulse edges, resulting in formation of the three-pulse ME signal. The ME amplitude is proportional to the number of nuclei in a Δx layer formed when the DW is displaced: $I_{ME} \sim \Delta x/L$, where L is the width of the excited section of the DW under the action of an RF pulse. These nuclei do not contribute in SPE formation due to the loss of phase coherence and, correspondingly, I_{SPE} is proportional the number of nuclei in the remaining part of excited by RF pulse DW section $I_{SPE} \sim (L - \Delta x)/L$. In this case, the jump-like change in the NMR frequency in the RCS at combined action of RF and MVP, must satisfy the condition $\Delta\omega'_j\tau_d \ll 1$, or, in other words, the precession period of the nuclei in the RCS $\Delta\omega'_j = (\Delta\omega^2 + \omega_1^2)^{1/2}$ should be larger as compared with τ_d . When the MVP is applied to the TPE in the interval between RF pulses, nuclei precess in the local HFF with a frequency $\omega_j = \gamma_n H_{HFF}$ and, therefore, the new condition $\omega_j\tau_d \ll 1$ should be fulfilled to observe an additional ME signal, which requires that a nanosecond duration of the MVP τ_d must be used, as in case of observing an inverse echo signal (Ignatchenko et al., 1963), which in our case is not satisfied. Therefore, the effect of MVP on TPE leads only to a decrease in the intensity of TPE, proportional to a DW displacement Δx : $I_{TPE} \sim (L - \Delta x)/L$, due to the loss of phase coherence of nuclei in this layer. These qualitative considerations make it possible to understand the obtained experimental dependences of the ME, SPE and TPE signals under the action of MVP.

The measurements were carried out on a phase-incoherent spin echo spectrometer (Gavasheli et al., 2022; Mamniashvili & Gegechkori, 2023) in the frequency range of 200–400 MHz at a temperature of 293 K. In the range of 200–400 MHz, a commercial Lecher-type generator with a two-wire line, including two inductors with different numbers of turns, was used. For pulse lengths in the range from 0.1 to 50 μs , the maximum amplitude of the RF field produced on the sample was about 3.0 Oe, and the front steepness was no worse than 0.15 μs . Receiver dead time $\sim 1 \mu s$.

The scheme of the experiment on pulsed magnetic action is given in (Gavasheli et al., 2022; Mamniashvili & Gegechkori, 2023).

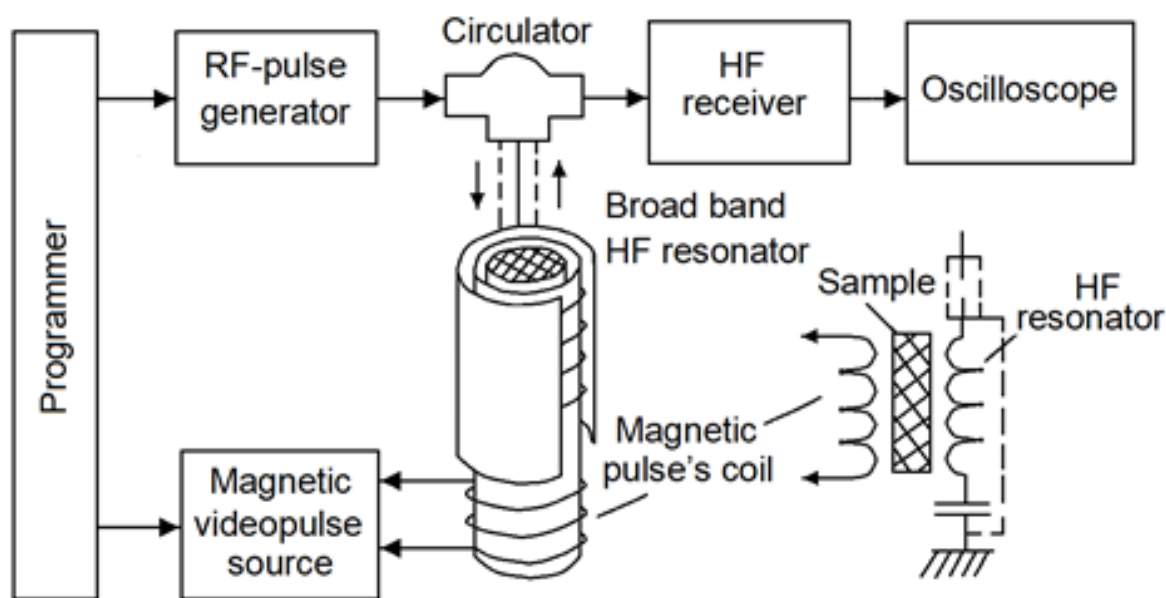


Figure7. NMR spectrometer setup

The MVP was created by a gated current stabilizer of adjustable amplitude and an additional copper coil, which made it possible to obtain magnetic field pulses of the order of 500 Oe for a sample size of ~ 10 mm.

Cobalt micropowders were obtained by the alloying method (Gavasheli et al., 2022; Mamniashvili & Gegechkori, 2023) with an average grain size of $\sim 10 \mu s$. Characteristic parameters of RF pulses: duration - a few microseconds, a delay between them - tens of microseconds, a carrier frequency of 213 MHz at $T = 293$ K coincides with the frequency of the nuclei in the centres of the DW of the face-centred cubic (fcc) phase of cobalt.

The oscillograms of the experiments are shown in Figure 8.

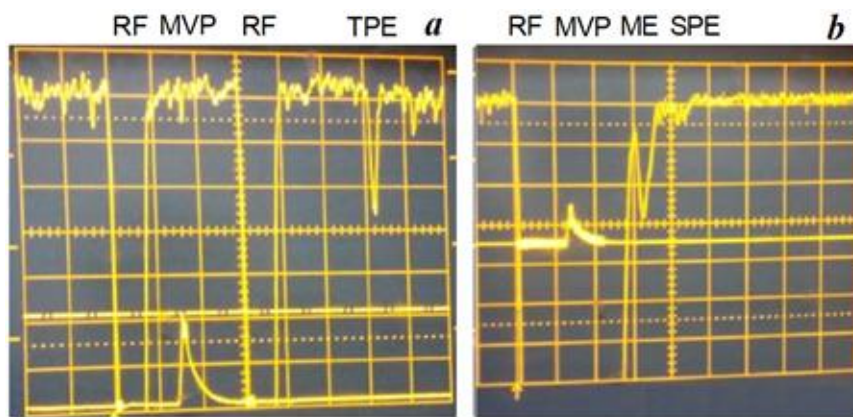


Figure 8. Oscilloscope of the TPE signal in cobalt (upper beam) and the wavemeter signal showing the position of RF and MVP pulses (lower beam) (a); oscilloscope of the ME and RPE signals in cobalt, the lower beam shows the duration and position of the RF pulse, as well as the position of the MVP (b).

The NMR spectrum of the studied cobalt sample is shown in Figure 9 a. Comparison of curves 1 and 4 in Figs. 9b indicates a much higher magnetic hardness of cobalt compared to lithium-zinc ferrite. Curves 2 and 3 in Figs. 9b demonstrate similar dependences of the relative intensity I/I_{max} of the TPE and ME signals on the magnetic field H_c , which reflects the same mechanisms of their formation (Mamniashvili et al., 2022). Figure 8 shows oscillograms explaining the scheme of the experiment and Figure 9b shows the dependences of the TPE on the MVP amplitude under the action of an external H_c field and the corresponding results for the ME.

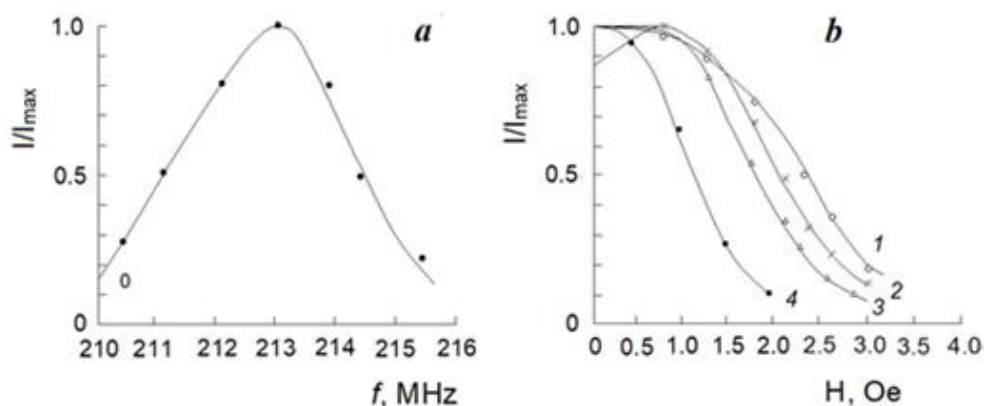


Figure 9. ^{59}Co NMR spectrum of the investigated Co micropowder (a) a change in the relative intensities I/I_{max} of echo signals in cobalt with increasing constant magnetic field H_c : curves 1, 2, 3 – TPE, SPE, and ME, respectively, 4 - TPE in lithium-zinc ferrite (b); $T=293\text{K}$.

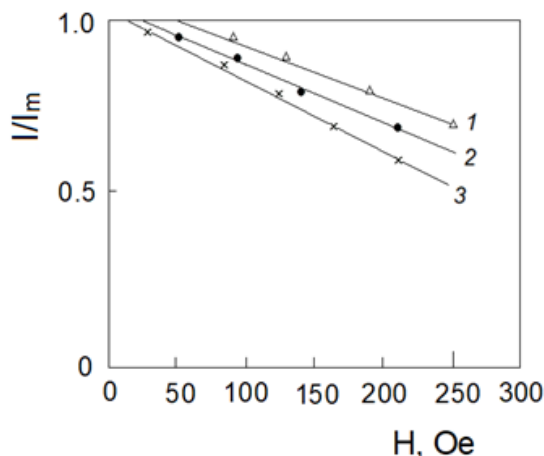


Figure 10. Dependence of the normalized TPE intensity I/I_m on the MVP amplitude H : 1-3 at $\tau_m = 1, 2,$ and $3 \mu\text{s}$, respectively.

Let us present the results of the study of the pinning force H_0 under the action of an additional MVP, depending on the duration of the MVP τ_m , on the TPE signals in a cobalt micropowder, Figure 10. Analysis of the obtained results in Figure 10 shows that in the case of cobalt the relation $A_m = H_0 \cdot \tau_m = \text{const}$, also holds according to which the MVP threshold area is constant for all MVP durations. This coincides with a similar conclusion for the MVP threshold area in the case of nickel ferrite, Figure 6.

It should be noted that for the first time such a relation was established in the NMR study of the pinning force H_0 of the ME signal dependence on τ_m (Gavasheli et al., 2022; Mamniashvili & Gegechkori, 2023) in cobalt. And A_m is the threshold area of the MVP, corresponding to the beginning of the displacement of the DW under the action of the MVP. The physical meaning of this result can be understood if we take into account that, according to the one-dimensional DW model (Konishi et al., 1976), the DW displacement x under the action of a short MVP with amplitude H and duration τ_m is determined by the relation

$$x = C \cdot H \cdot \tau_m,$$

Where C is a constant characteristic of the material under study. Thus, the same displacement of the DW corresponds to any of the threshold values of the MVP, and it is natural to associate it with the width of the potential well in which the DW is located in the initial state. We also note that a similar relationship between H and τ_m was established in the study of Permalloy films by the Kerr magneto-optical method (Bartran & Bourne, 1973).

Let us further investigate the dependence of H_0 on the magnitude of the external magnetic field H_e at a fixed MVP duration $\tau_m = 1 \mu\text{s}$.

The results obtained by two alternative methods show an increase in the pinning force in cobalt with increasing H_e in accordance with (Pleshakov et al., 2016), but in a larger range (up to 3 kOe) compared to 1 kOe in lithium-zinc ferrite [5] and confirm the possibility of studying the force pinning of H_0 in cobalt micropowders by two alternative NMR methods using additional MMI. In contrast to [5], an increase in the pinning force in cobalt is observed in a wider range of external constant magnetic field H_e due to the higher magnetic hardness of cobalt compared to lithium-zinc ferrite (~3 kOe in cobalt compared to ~1 kOe in lithium-zinc ferrite).

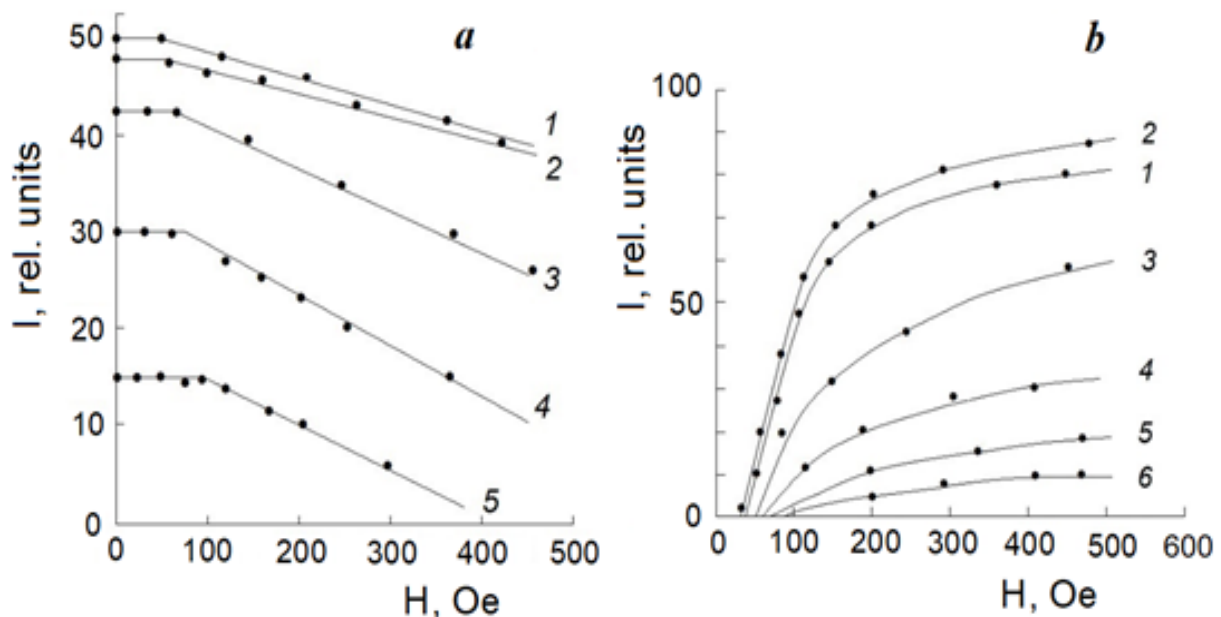


Figure 11. Dependences of the TPE intensity on the MVP amplitude in cobalt in the interval between RF pulses at $H_e = 0$ (1), 0.8 (2), 1.9 (3), 2.3 (4), and 3 kOe (5) (a) and the intensity ME on the MVP amplitude in cobalt at $H_e = 0$ (1), 0.8 (2), 1.3 (3), 2.3 (4), 2.6 (5), and 2.8 kOe (6).

Based on the data in Fig. 11, it is possible to construct the dependence of the pinning force H_0 on the magnitude of the external field H_e , Figure 12.

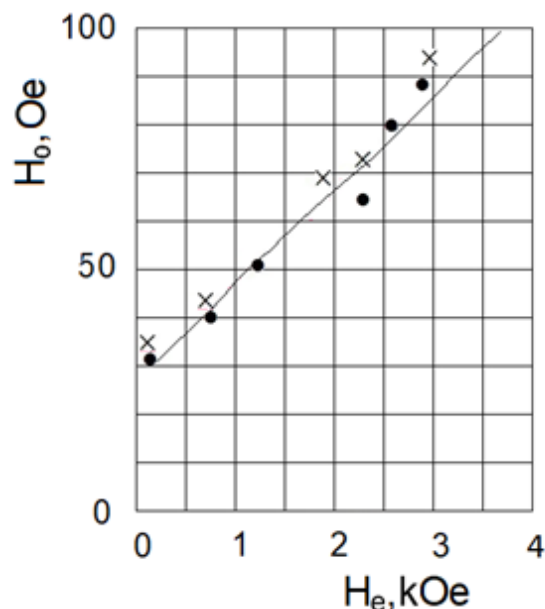


Figure 12. Dependence of the pinning force H_0 on the magnitude of the external constant magnetic field H_e on the threshold of the ME signal generation (x) and the influence of the MVP on the TPE amplitude (•).

Thus, it has been established that up to external fields ~ 3 kOe, a linear dependence of H_0 on H_e is observed. This indicates that, at higher H_e , the DWs are distributed over positions corresponding to the parameters of the potential walls providing stronger pinning. We also note a feature of the data in Figure 11, which consists in the fact that the rate of suppression of the TPE signal increases with increasing H_e , in contrast to that observed in lithium ferrite (Pleshakov et al., 2016), which is due to the differences in the NMR properties of cobalt and lithium ferrite noted above (Mamniashvili et. al., 2021).

Conclusions

It is shown that the excitation of nuclear spin echo signals in combination with a magnetic video-pulse is a convenient method for evaluation the domain wall pinning field in magnetic materials on example of a lithium-zinc sample. Two different methods were applied to evaluate the domain wall pinning in a lithium-zinc ferrite. In the first case, the pinning of domain walls was measured by the action of magnetic video-pulse on a two-pulse echo signal, and in the second one, the pinning was measured at the combined action of magnetic video-pulse and RF pulses on the nuclear spin system in domain walls in the process of formation of a single-pulse echo, by means of generation of the so-called magnetic echo signal.

Qualitative considerations are presented making it possible to understand the obtained experimental dependences of the single-pulse, magnetic and two-pulse echo signals under the action of a magnetic video-pulse.

In the present work, for the first time, the pinning force of domain walls was studied by the NMR two-pulse spin-echo method under the action of an additional magnetic video-pulse in cobalt. It was shown that the pinning value H_0 is inversely proportional to the length of the magnetic video-pulse τ_m . In addition, the area of the magnetic video pulse turned out to be constant for all threshold durations of the magnetic video pulse.

The dependence of the pinning force H_0 on the external constant magnetic field H_e is studied. It is shown that up to ~ 3 kOe there is a linear dependence of H_0 on H_e . This indicates that as the H_e increases the domain walls are distributed over sites corresponding to the stronger pinning centers.

The degree of pinning (pinning force) of domain walls in cobalt micropowder has been studied by two alternative NMR methods: by the action of a magnetic video pulse on a two-pulse echo and by the threshold for generating of the magnetic echo signal under the action of an additional magnetic video-pulse. A linear dependence of the pinning force on the amplitude of the magnetic video pulse is established in a wider range of the external magnetic field (up to ~ 3 kOe) compared to the softer lithium-zinc ferrite (observed up to 1 kOe).

Scientific Ethics Declaration

The authors declare that the scientific ethical and legal responsibility of this article published in EPSTEM journal belongs to the authors.

Acknowledgements or Notes

* This article was presented as oral presentation at the International Conference on Basic Sciences, Engineering and Technology (www.icbasnet.net) held in Marmaris/Turkey on April 27-30, 2023.

* This work was supported by Shota Rustaveli National Science Foundation of Georgia (Grant # STEM-22-1339).

References

- Bartran, D., & Bourne, H. (1973). Domain wall velocity and interrupted pulse experiments. *IEEE Transactions on Magnetics*, 9(4), 609-613.
- Doroshev, V. D., Klochan, V. A., Kovtun, N. M., & Seleznev, V. N. (1972). The effect of dipole and anisotropic hyperfine fields on NMR of Fe⁵⁷ in lithium ferrite Li_{0.5}Fe_{2.5}O₄. *Physica Status Solidi A*, 9(2), 679-689.
- Galt, J. K. (1954). Motion of individual domain walls in a nickel-iron ferrite. *Bell Labs Technical Journal*, 33(5), 1023-1054.
- Gavasheli, T. A., Mamniashvili, G. I., Shermadini, Z. G., Zedginidze, T. I., Petriashvili, T. G., Gegechkori, T. O., & Janjalia, M. V. (2020). Investigation of the pinning and mobility of domain walls in cobalt micro- and nanowires by the nuclear spin echo method under the additional influence of a magnetic video pulse. *Journal of Magnetism and Magnetic Materials*, 500, 166310.
- Gavasheli, T., Gegechkori, T., Mamniashvili, G., & Gvedashvili, G. (2021). NMR spin echo study of domain wall pinning in lithium ferrite in combination with an additional magnetic video-pulse. *Proceedings of the XXVI International Seminar/Workshop on Direct and Inverse Problems of Electromagnetic and Acoustic Wave Theory (DIPED-2021)*, (pp. 199-202). IEEE.
- Gavasheli, T., Mamniashvili, G., Ghvedashvili, G., & Gegechkori, T. (2022). NMR spin-echo study of the domain wall pinning in cobalt micropowders. *Proceedings of the 2nd Ukrainian Microwave Week (UkrMW)*, (pp. 405-409). IEEE.
- Ignatchenko, V. A., Mal'tsev, V. K., Reihgardt, A. E., & Tsifrinvich, V. I. (1983). New mechanism for formation of nuclear-spin echo. *JETP Letters*, 37(9), 520-522.
- Konishi, S., Mizuno, K., Watanabe, F., & Narita, K. (1976). Domain wall displacement under pulsed magnetic field. *AIP Conference Proceedings*, 34(1), 145-147.
- Mamniashvili, G. I., Gegechkori, T. O., Akhalkatsi, A. M., & Gavasheli, T. A. (2015). On the role of the hyperfine field anisotropy in the formation of a single-pulse NMR spin echo in cobalt. *Journal of Superconductivity and Novel Magnetism*, 28(3), 911-916.
- Mamniashvili, G., Zviadadze, M., Gegechkori, T., & Shermadini, Z. (2016). NMR spectroscopy of magnets using arbitrary number and duration radio-frequency pulses. *International Journal of Trend in Research and Development*, 3(2), 434-473.
- Mamniashvili, G. I., Gegechkori, T. O., & Gavasheli, Ts. A. (2021). Study of the nature of the NMR signal in lithium ferrite upon exposure to a low-frequency magnetic field. *Physics of Metals and Metallography*, 122(9), 841-846.
- Mamniashvili, G., Gegechkori, T., Janjalia, M., & Gogishvili, P. (2022). Investigation of the single-pulse NMR echo origin in cobalt using additional magnetic video-pulses. *Magnetic Resonance in Solids*, 24, 22102.
- Mamniashvili, G. I., & Gegechkori, T. O. (2023). Investigation of the characteristics of domain wall fixation centers in cobalt by nuclear magnetic resonance. *Journal of Applied Spectroscopy*, 89(6), 1076-1079.
- Pleshakov, I. V., Popov, P. S., Kuz'min, Yu. I., & Dudkin, V. I. (2016). NMR study of domain wall pinning in a magnetically ordered material. *Technical Physics Letters*, 42(1), 59-62.
- Rassvetalov, L. A., & Levitski, A. B. (1981). Influence of a pulsed magnetic field on the nuclear spin echo in some ferromagnets and ferrimagnets. *Soviet Physics, Solid State*, 23(11), 3354-3359.
- Shmyreva, A. A., Matveev, V. V., & Yurkov, G. Y. (2016). Nuclear magnetic resonance in magnetic nano-materials as an effective technique to test and/or to certificate local magnetic properties. *International Journal of Nanotechnology*, 13(1-3), 126-135.
- Turov, E. A., & Petrov, M. P. (1972). *Nuclear magnetic resonance in ferro- and antiferromagnets*. New York, NY: Halsted (Wiley).

Wurmehl, S., & Kohlhepp J. T. (2008). Nuclear magnetic resonance studies of materials for spintronic applications. *Journal of Physics D: Applied Physics*, 41(17).

Author Information

Tsisana Gavasheli

Ivane Javakishvili Tbilisi State University
Tbilisi, Georgia
Contact e-mail: tsismari.gavasheli@tsu.ge

Grigor Mamniashvili

Ivane Javakishvili Tbilisi State University
Tbilisi, Georgia

Tatiana Gegechkori

Ivane Javakishvili Tbilisi State University
Tbilisi, Georgia

To cite this article:

Gavasheli.T., Mamniashvili G., & Gegechkori T., (2023). NMR spin echo study of domain wall pinning in magnets in combination with an additional magnetic video-pulse, *The Eurasia Proceedings of Science, Technology, Engineering & Mathematics (EPSTEM)*, 22, 348-358.